Parton Showers, Event Shapes, Jet Algorithms

So far in this course, we have discussed two approaches to QCD radiation. First, we saw that most of the radiation is emitted in directions collinear with the initial and final particles. The emitted particles are spaced out uniformly in $\log p_T$ (to the extent that α_s can be taken to be constant). We saw that these emissions affect the longitudinal distribution of the initial and final partons, and that these effects can be accounted by solving the Altarelli-Parisi equations.

We also saw that it is possible to make a detailed accounting of QCD corrections to a fixed order in perturbation theory. That accounting requires computation of real and virtual corrections and careful treatment of infrared divergences. The full computation of real corrections generates some new effects - p_T distributions for initial and final particles, and radiation of additional jets of hadrons.

These effects are reflected in the data. Fig. p.2 shows an e^+e^- annihilation event at $\sqrt{s} = m_Z$ similar to those I showed in earlier lectures, with two well-defined jets. However, in Figs. p.3 you see an event with 3 jets, and Figs. p.4 shows an event with 4 jets. In these latter two events, the jets are clearly being broadened by QCD radiation, and the division of the jets from one another is not unambiguous. In principle, we could arbitrarily divide these events into 3 jets and measure the energy of each. The result of this is shown in Figs. p. 5. The energy of the third jet has the form

$$\frac{1+(1-z)^2}{z}$$

that we should have expected.

These considerations raise some questions:

- Can we predict the shapes of events generated by QCD?
- How many jets do these events contain? How do we divide an event into jets?
- How do we make quantitative comparisons of ~~event~~ shapes to QCD predictions?

In this lecture, I will discuss three approaches to these problems:

① Simulation of QCD events by parton showers.

② Characterization of events by event shape observables.

③ Identification of jets by jet algorithms.

First, let's discuss parton showers. These are models that take into account all orders of collinear parton emissions and attempt to construct the complete final state that results. The general-purpose QCD event generators PYTHIA, HERWIG, and SHERPA are built around parton showers.

Consider first the parton shower generated by a final state parton:

According to the Altarelli-Parisi equation, the probability of emitting a collinear parton is given by

non-δ-fcn part of $\mathbb{P}_{j\leftarrow i}$

$$\frac{d}{d\log Q}(\text{Probability})_{j\leftarrow i} = \frac{\alpha_s(Q)}{\pi}\int dz\ \hat{\mathbb{P}}_{j\leftarrow i}(z)$$

It is straightforward to simulate this as a stochastic process. Take steps in Q and, in each step, decide (probabilistically) whether a parton should be emitted. If we decide to generate the branching $i \to jk$, we assign

$$p_j^{\parallel} = z\,p_i \qquad p_k^{\parallel} = (1-z)\,p_i$$

and assign the p_T's relative to the direction of p_i by

$$Q^2 = \frac{p_T^2}{z(1-z)}$$

The parton i must be put off-shell so that $p_i^2 = Q^2$. To conserve energy-momentum, transfer some momentum from a third particle

$$i \longleftrightarrow l \qquad \hat{s}$$

$$\Downarrow$$

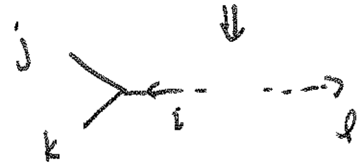

$$p_l = \frac{\hat{s}-Q^2}{2\sqrt{\hat{s}}}$$

In PYTHIA, for example, l is taken to be the parton created with i in the previous branching. Continue in this way until Q decreases to the infrared cutoff scale Q_{min}. Then each approximately collinear parton is generated with finite p_T in approximately the correct distribution, and we can consider the resulting parton configurations to be a QCD model of event shapes.

There is a more automatic way to choose the Q values for branching. Let

$$t = \log \frac{Q_0}{Q}$$

be the evolution variable for the shower. t runs from 0 to $t_{max} = \log Q_0/Q_{min}$. Consider a parton i created in a branching at t_i. The probability $\mathbb{P}_i(t)$ that this parton has not branched again before t is the solution of

$$\frac{d}{dt}\mathbb{P}_i(t) = -\left[\frac{\alpha_s(t)}{\pi}\int dz \sum_j \hat{P}_{j\leftarrow i}(z)\right]\mathbb{P}_i(t)$$

with initial condition $\mathbb{P}_i(t_i) = 1$. Then

$$\mathbb{P}_i(t) = \exp\left[-S_i(t;t_i)\right]$$

where $S_i(t;t_i) = \int_{t_i}^{t} dt \int dz \sum_j \hat{P}_{j\leftarrow i}(z)$ "Sudakov factor"

[To make this finite, the z integral may need an IR cutoff at small z.]

The probability that the first emission is at t is

$$\frac{d\mathbb{P}_i}{dt}\, dt$$

So, choose a random number R $\quad 0 \le R \le 1$, set

$$R = e^{-S_i(t;t_i)}$$

and solve this equation for t. This algorithm generates the correct distribution of emissions.

There are a number of ambiguities in this algorithm that are resolved in different ways in different programs. I have already noted that prescriptions are needed for implementing energy-momentum conservation and for providing IR cutoffs on the dQ and dt and the dz integrals. The specific ordering variable also has some freedom of choice. In the discussion above, I have chosen Q to be the shower ordering variable ("virtuality ordering"). In PYTHIA, p_T is taken as the ordering variable and Q is reconstructed by $Q^2 = p_T^2/z(1-z)$. In HERWIG, the lab-frame angle is used as the ordering variable, so that we obtain an angular-ordered shower.

This last choice seems odd, but there is a strong argument for angular ordering, due originally to Mueller. In the parton shower algorithm described above, every parton showers independently. However, in QCD, the pattern of soft radiation is affected by interference. The simplest example of this is seen in $e^+e^- \to q\bar{q}$. The first branching produces a color-singlet QCD dipole

Then we might expect that gluons emitted outside the $q\bar{q}$ cone see a color singlet and, thus, destructive interference, while gluons emitted at small angles see constructive interference

destructive:

constructive:

It is not so hard to show this analytically. Let p_1, p_2, k be the momenta of the quark, antiquark, and gluon. In the soft gluon limit

$$\int d\sigma \sim \frac{\alpha_s}{\pi} \int \frac{dk}{k} \int d\Omega_k \; \frac{p_1 \cdot p_2}{p_1 \cdot \hat{k} \; p_2 \cdot \hat{k}}$$

where $\hat{k}$ is a unit vector in the direction of k.

$$\sim \frac{\alpha_s}{\pi} \int \frac{dk}{k} \int d\Omega_k \; \frac{1-\cos\theta_{12}}{(1-\cos\theta_{1k})(1-\cos\theta_{2k})}$$

Now we can rewrite

$$\frac{1-\cos\Theta_{12}}{(1-\cos\Theta_{1k})(1-\cos\Theta_{2k})} = \frac{1}{2}\left[\frac{1-\cos\Theta_{12}}{(1-\cos\Theta_{1k})(1-\cos\Theta_{2k})} - \frac{1}{1-\cos\Theta_{2k}} + \frac{1}{1-\cos\Theta_{1k}}\right]$$

$$+ \quad (1\leftrightarrow 2)$$

$$= \frac{1}{2}\left[\frac{\cos\Theta_{1k}-\cos\Theta_{12}}{1-\cos\Theta_{2k}} + 1\right]\frac{1}{1-\cos\Theta_{1k}} + (1\leftrightarrow 2)$$

The term $\frac{1}{1-\cos\Theta_{1k}}$ is the collinear singularity as $\hat{k}\to\hat{1}$. Let's average this term over the orientation of k relative to P.

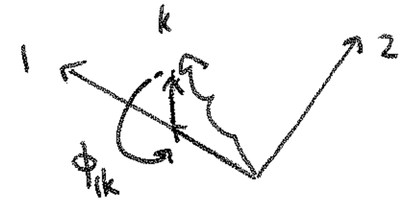

$$\cos\Theta_{2k} = \cos\Theta_{1k}\cos\Theta_{12} + \sin\Theta_{1k}\sin\Theta_{12}\cos\phi_{1k}$$

then

$$1-\cos\Theta_{2k} = a - b\cos\phi_{1k}$$

where $a = 1-\cos\Theta_{1k}\cos\Theta_{12}$ $\quad b = \sin\Theta_{1k}\sin\Theta_{12}$

Now compute the average of the above expression over ϕ_{1k}. For this we need to compute

$$\int\frac{d\phi_{1k}}{2\pi}\frac{1}{1-\cos\Theta_{2k}} = \int\frac{d\phi_{1k}}{2\pi}\frac{1}{a-b\cos\phi_{1k}}$$

To evaluate the integral, let $\quad z = e^{i\phi_{1k}} \quad \cos\phi_{1k} = \frac{z+z^{-1}}{2}$

$$= \oint\frac{dz}{z}\frac{(-i)}{2\pi}\frac{1}{a-\frac{b}{2}\left(z+\frac{1}{z}\right)} = -\frac{2}{b}\oint\frac{dz}{2\pi i}\frac{1}{\left(z^2-\frac{2a}{b}z+1\right)}$$

The integrand has poles at $\quad z_\pm = \frac{a}{b} \pm \sqrt{\left(\frac{a}{b}\right)^2-1}$

We can do the integral by contours, picking up the pole at z_-

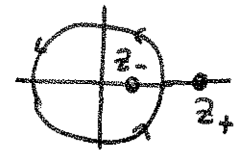

$$\int \frac{d\phi_{1k}}{2\pi}\, \frac{1}{1-\cos\phi_{1k}} = \frac{2}{b}\, \frac{1}{|z_+ - z_-|} = \frac{1}{[a^2-b^2]^{1/2}}$$

and

$$a^2-b^2 = 1 - 2\cos\theta_{1k}\cos\theta_{12} + \cos^2\theta_{1k}\cos^2\theta_{12} - \sin^2\theta_{1k}\sin^2\theta_{12}$$

$$= \left(1 - \cos^2\theta_{1k} - \cos^2\theta_{12} + \cos^2\theta_{1k}\cos^2\theta_{12}\right) - \sin^2\theta_{1k}\sin^2\theta_{12} \quad = 0!$$

$$+ \cos^2\theta_{1k} - 2\cos\theta_{1k}\cos\theta_{12} + \cos^2\theta_{12}$$

$$= (\cos\theta_{1k} - \cos\theta_{12})^2$$

so

$$\int \frac{d\phi_{1k}}{2\pi}\, \frac{1}{2}\left[\frac{\cos\theta_{1k} - \cos\theta_{12}}{1-\cos\theta_{2k}} + 1\right]\frac{1}{1-\cos\theta_{1k}}$$

$$= \frac{1}{2}\underbrace{\left[\frac{\cos\theta_{1k} - \cos\theta_{12}}{|\cos\theta_{1k} - \cos\theta_{12}|} + 1\right]}\frac{1}{1-\cos\theta_{1k}}$$

this factor $=$ 1 if k is inside the cone formed by p_1, p_2

0 if k is outside this cone.

So the amplitude for soft radiation cancels unless the emission obeys angular ordering.

This angular ordering is good thing, allowing QCD showers to model some part of the QCD interference. As I have said, angular ordering is automatic in the HERWIG shower. In PYTHIA, emissions that violate angular ordering are vetoed.

Parton showers from initial-state partons bring some further complications.

Again, we work from the hard process outward, from the hard-scattering scale Q_0 to the IR scale Q_{min}. Now Q and p_T have the relation

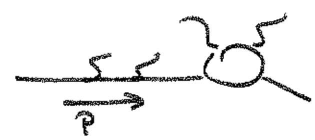

$$Q^2 = \frac{p_T^2}{(1-z)}$$

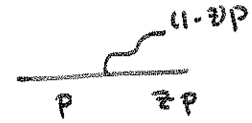

but this is a relatively trivial change. A more nontrivial question is, how do we choose the branching points in this case? We need to take ~~into~~ account both the form of the splitting function and the form of the pdf. We want, in particular, to disfavor reactions that require moving to regions where the pdf is small.

Let a parton i originate at $t = t_i$

~~The probability that~~ this parton enters the reaction is proportional to

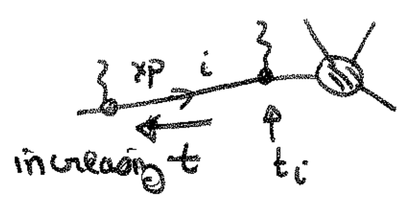

$$f_i(x, t_i)$$

As we go to higher t (lower Q) the differential probability that i came from an earlier radiation at t is

$$\frac{dt \; \frac{\alpha_s(t)}{\pi} \int \frac{dz}{z} \; \hat{P}_{i\leftarrow j}(z) \; f_j\left(\frac{x}{z}, t\right)}{f_i(x,t)}$$

Now, $$\frac{\partial}{\partial t} f_i(x,t) = \frac{\alpha_s}{\pi} \int \frac{dz}{z} \; P_{i\leftarrow j}(z) \, f_j\left(\frac{x}{z}, t\right)$$

but $\hat{P}$ has only the emission $\sim P$, not the $\delta(z-1)$.

$$P_{i\leftarrow j}(z) = \hat{P}_{i\leftarrow j}(z) - \delta(z-1)\int dz' \sum_k P_{k\leftarrow i}(z')\,\delta_{ij}$$

so

$$\frac{\alpha_s(t)}{\pi}\int \frac{dz}{z}\,\hat{P}_{i\leftarrow j}(z) f_j\left(\frac{x}{z},t\right)$$

$$= \frac{\partial}{\partial t} f_i(x,t) + f_i(x,t)\,\frac{\partial}{\partial t} S_i(t;t_i)$$

where the Sudakov factor S_i was defined on p. 4. The probability that there were no emissions from t_i to t obeys:

$$\frac{d}{dt}\mathbb{P}_i(t) = -\left[\frac{\frac{\partial}{\partial t} f_i(x,t)}{f_i(x,t)} + \frac{\partial}{\partial t} S_i(t)\right]\mathbb{P}_i(t)$$

$$= -\frac{\partial}{\partial t}\log\left[f_i(x,t)\,e^{S_i(t)}\right]\mathbb{P}_i(t)$$

for which the solution is

$$\mathbb{P}_i(t) = \frac{f_i(x,t_i)}{f_i(x,t)}\,e^{-S_i(t;t_i)}$$

To find the next branching t we solve

$$R = \frac{f_i(x,t_i)}{f_i(x,t)}\,e^{-S_i(t;t_i)}$$

That is, if the pdf at x ~~decreases~~ with Q (increases with t)

that we are more likely to branch at a larger t, and vice versa. This is the method of backwards evolution, invented by Sjöstrand.

Now that we understand, at least in principle, how parton showers work, I will go on to discuss event shapes. I will show comparisons of data both to order-by-order QCD predictions and to parton shower event generators.

First, I would like to discuss "event shape variables" that quantify how jetty an individual event might be. Jets were originally discovered in the Mark I experiment at SLAC, at energies of 3 – 7.4 GeV in e^+e^- annihilation to hadrons, by Gail Hanson. At these low energies, the jet structure of final states is not at all obvious. Hansen tried to tease it out by using a quantity called the sphericity tensor

$$S^{ij} = \frac{\sum_a p_a^i p_a^j}{\sum_a |\vec{p}_a|^2} \qquad a = \text{particle (track)}$$

The largest eigenvector of S^{ij} would correspond to the jet axis. Let p_{aT} be the component of $\vec{p}_a$ orthogonal to this "sphericity axis". Then Hansen defined the sphericity by

$$S = \frac{3}{2}\,\frac{\sum_a p_{Ta}^2}{\sum_a p_a^2} = \min_{\text{axes } \hat{n}} \ \frac{3}{2}\,\frac{\sum_a |p_{Ta} \text{ to } n|^2}{\sum_a |p_a|^2}$$

For an isotropic (spherical) event $\langle p_T^2 \rangle = \frac{2}{3}\langle p^2 \rangle$, so $S \to 1$. For a jet-like event $S \to 0$. Figs. p. 6 shows a comparison of the distribution of S at different energies to a model with phase space emission (dashed curve) and a model with particle emission along a definite jet axis, with limited p_T with respect to this axis. The two distributions are indistinguishable at 3 GeV but become distinctly different at higher energies.

There is a problem with the sphericity variable, though. It has no definite prediction in QCD. In QCD, there is essentially an infinite probability to have a collinear splitting

$$\underset{p}{\longrightarrow} \quad \Rightarrow \quad \begin{array}{c} zp \\ \longrightarrow \\ \rightsquigarrow \\ (1-z)p \end{array}$$

This splitting changes the value of an ingredient of S

$$\mathbf{p}_a^2 \to [z^2 + (1-z)^2]\, p_a$$

It would be much better to average a quantity with the property that it is unchanged by a collinear splitting. Then the average of this quantity will have a definite value in QCD perturbation theory. Such a quantity is called "infrared safe".

Farhi proposed an infrared safe replacement for sphericity, now called "thrust"

$$T = \max_{\hat{n}} \frac{\sum_a |\vec{p}_a \cdot \hat{n}|}{\sum_a |\vec{p}_a|}$$

For this variable, when a parton splits into a collinear pair of partons, it gives the same contribution to T. Another infrared-safe event shape variable is the Energy-Energy Correlation Function of Basham, Brown, Ellis, and Love:

$$\frac{1}{\sigma_0} \frac{d\sigma}{d\cos\chi} = \sum_{ab} \frac{E_a E_b}{s} \delta(\hat{p}_a \cdot \hat{p}_b - \cos\chi)$$

I would now like to compute the thrust distribution in $e^+e^- \to$ hadrons in QCD. For a linear (2-parton) configuration, $T = 1$, the maximum value. The minimum value of thrust, found for an isotropic event, is

$$T = \langle |\cos\theta| \rangle = \int_{-1}^{1} \frac{d\cos\theta}{2} |\cos\theta| = \frac{1}{2}$$

What is the thrust of a 3-parton configuration as in

$e^+e^- \to q\bar{q}g$. As in our earlier discussion, we can view the final state in the <u>event</u> <u>plane</u>

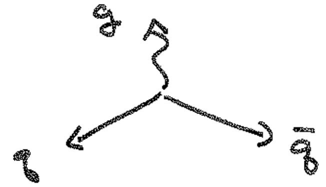

with variables $x_1 = \frac{2E_q}{E_{cm}}$ $\quad x_2 = \frac{2E_{\bar{q}}}{E_{cm}}$ $\quad x_3 = \frac{2E_g}{E_{cm}}$

$x_1+x_2+x_3 = 2$. To maximize T, put the thrust axis along the direction of the most energetic parton. Then, e.g., if

$x_1 > x_2, x_3$

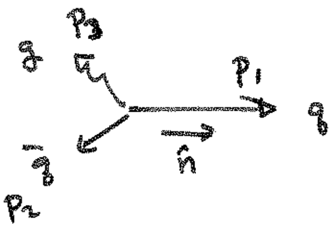

$$\hat{n}\cdot\vec{p}_1 = -\hat{n}\cdot\vec{p}_2 - \hat{n}\cdot\vec{p}_3$$

so that

$$T = \frac{2x_1}{2} = x_1$$

Notice that as $x_1 \to 1$
$T \to 1$ = (thrust of a 2-jet configuration)

More generally,

$$T = \max\{x_1, x_2, x_3\}$$

Recall that $x_1\ x_2$ are integrated over the region

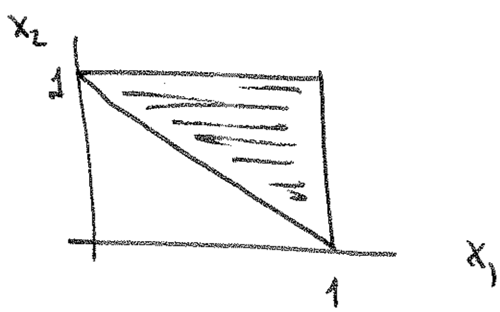

This triangle splits into three regions :

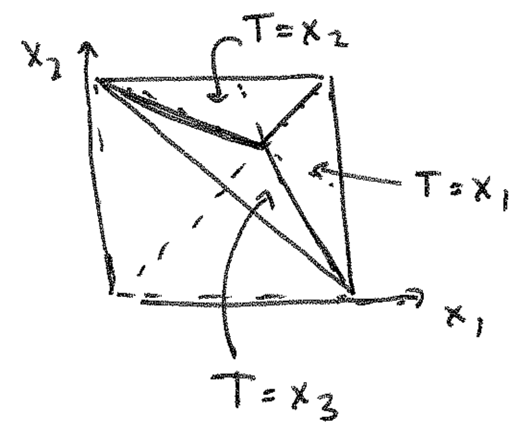

Recall that the 3-jet cross section is

$$\frac{d\sigma}{dx_1 dx_2} = \sigma_0 \cdot \frac{2\alpha_s}{3\pi} \cdot \frac{x_1^2 + x_2^2}{(1-x_1)(1-x_2)}$$

We can now find the thrust distribution by ~~integrating~~ this formula over each of the three regions:

$$\frac{d\sigma}{dT} = \sigma_0 \cdot \frac{2\alpha_s}{3\pi} \cdot \Big\{ \int_{2(1-x_1)}^{x_1} dx_2 \left. \frac{x_1^2 + x_2^2}{(1-x_1)(1-x_2)} \right|_{x_1 = T}$$

$$+ \int_{2(1-x_2)}^{x_2} dx_1 \left. \frac{x_1^2 + x_2^2}{(1-x_1)(1-x_2)} \right|_{x_2 = T}$$

$$+ \int_{2(1-x_3)}^{x_3} dx_1 \left. \frac{x_1^2 + (2-x_1-x_3)^2}{(1-x_1)(x_1+x_3-1)} \right|_{x_3 = T} \Big\}$$

The ~~integrals~~ are more or less straightforward. The result is

$$\frac{d\sigma}{dT} = \sigma_0 \cdot \frac{2\alpha_s}{3\pi} \left\{ \frac{2(3T^2 - 3T + 2)}{T(1-T)} \log \frac{2T-1}{1-T} - \frac{3(3T-2)(2-T)}{(1-T)} \right\}$$

Notice that $\frac{d\sigma}{dT}$ is singular as $T \to 1$, as we might have expected. Notice also that $\frac{d\sigma}{dT} \to 0$ as $T \to 2/3$, which is the smallest value possible for a 3-parton system. The shape is

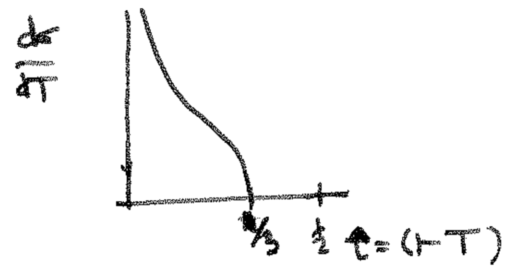

Values of T down to $\frac{1}{2}$ can be achieved in 4-parton configurations

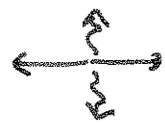

so order α_s^2 corrections fill in the region between $\tau = \frac{1}{3}$ and $\tau = \frac{1}{2}$, $\tau = (1-T)$.

Figs p.7 shows a comparison of the $\tau = (1-T)$ distribution measured by the SLD experiment at $\sqrt{s} = m_Z$ to the prediction from PYTHIA and HERWIG. Figs p.8 shows a more direct comparison of $\langle\tau\rangle$ and several other event shape variables to QCD predictions. The averages are shown as a function of $\sqrt{s}$. In perturbative QCD, we would expect

$$\langle(1-T)\rangle \sim \alpha_s(Q) \sim \frac{1}{\log Q}$$

and this general trend is seen in the figure. However, one obtains a much better fit at low Q by adding a power-law correction

$$\langle (1-T) \rangle = (QCD) + \frac{0.9\ \text{GeV}}{Q}$$

Such a term could arise from non-perturbative corrections. The sum of these terms is the solid line in Figs p.8. This non-perturbative effect is well modelled by the parton-shower event generators.

Event-shape variables still give a relatively crude picture of the form of the event. As an alternative, we might like to count jets. How can we do this?

To form jets, we associate tracks into clusters. The simplest algorithm to do this is the <u>JADE algorithm</u>: Consider the set of final-state particles $\{a\}$. For each pair of particles a, b, compute

$$y_{ab} = \frac{(p_a + p_b)^2}{s}$$

Choose the pair with the smallest value of y_{ab}, alternatively, the smallest invariant mass, and combine them into a single composite particle. Continue, until, for all (ab)

$$y_{ab} > y_{cut}$$

The composite particles at this stage are the jets in the event.

Notice that the number of jets depends on the choice of y_{cut} or of the minimum invariant mass $m_{min} = (y_{cut}\, s)^{\frac{1}{2}}$.

This is not a problem. When we compare to predictions from perturbative QCD, these predictions also depend on a minimum invariant mass. In fact, if α_s were constant, the collinear radiation of partons would be scale-invariant and would generate a fractal. The number of clusters in this fractal would depend on the cutoff scale. In real perturbative QCD, the same logic applies if $m_{min} >$ GeV.

In fact, it is ~~interesting~~ to compare the number of jets in $e^+e^- \to$ hadrons events at fixed $\sqrt{s}$ as a function of y_{cut}. Figs. p. 9 and 10 illustrate such a comparison for OPAL data at $\sqrt{s} = m_Z$. Figs p. 9 shows the QCD side. A parton shower algorithm is used to generate a quark-gluon final state. These quarks and gluons are clustered to given y_{cut}. The figure shows the fraction of 2-, 3-, 4- jet events. For large y_{cut}, almost all events are 2-jet; at smaller values, higher numbers of jets are revealed. The solid and dotted curves show the effects of hadronization and the effect of the particle detector. Figs. p. 10 (left side) shows the comparison of the final curves to the OPAL data. (Figs. p. 10 (right side) shows the comparison to $O(\alpha_s^2)$ QCD.) The correctness of the evolution of these curves with y_{cut} tests the validity of the Altarelli-Parisi equation.

Most studies of jets in e^+e^- annihilation use variants of the JADE algorithm. However, there is another algorithm that is sometimes used. In their text, Ellis, Stirling and Webber point out that the JADE algorithm sometimes gives counter intuitive results for jet combinations. Consider, for example, the 4-parton event

with double soft radiation. The JADE algorithm would often combine 3+4 first, and then the event would be interpreted as a 3-jet event. A more intuitive result would be to combine (3+1), (4+2) to form a 2-jet event. This is the result if we use the jet criterion

$$\hat{y}_{ab} = 2 \frac{\min(E_a^2, E_b^2)(1-\cos\theta_{ab})}{s}$$

The use of $\hat{y}_{ab}$ is called the "k_T algorithm".

Before we move on to hadron collider events, I would like to highlight one more aspects of event shapes in e^+e^-. Figs. p. 11 shows the energy flow and the particle flow as a function of the angle ϕ in the event plane for events recorded by the JADE detector at $Q = 29$-36 GeV. The coordinate system is one that puts the most energetic jet at $\phi = 0$ and chooses the ϕ direction as the direction from the first jet to the second:

$E_1 > E_2 > E_3$

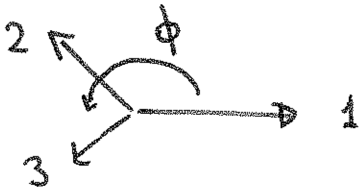

The dotted curve is the prediction of a model in which there are three initial partons that fragment independent to hadrons. The particle flow is depleted between jets 1 and 2 and enhanced between jets 2 and 3. In $e^+e^- \to q\bar{q}g$, the jet of lowest energy is usually the gluon, so

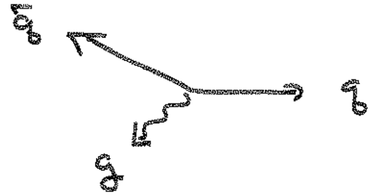

the depletion of energy between 1+2 and the enhancement in other regions is just the prediction of QCD coherence. In HERWIG, this effect is modelled by angular ordering. In PYTHIA, it is modelled by the hadronization algorithm, which uses a *color string* that runs from $\bar{q}$ to g to q.

Let's finally discuss event shapes in hadron-hadron collisions. We cannot simply apply the JADE algorithm to count jets. Many particles in the event are radiated into the region of *large* $|\eta|$ where they cannot be measured. The *underlying event*, the soft hadrons resulting from the proton-proton interaction, adds unrelated particles in the jet regions. So we need a different sort of jet algorithm.

The Tevatron experiments define jets in terms of the variables (p_T, η, ϕ). There are two ways to do this. The first is a cone algorithm. We draw a circle in the $\eta\phi$ plane for each cluster of p_T deposition:

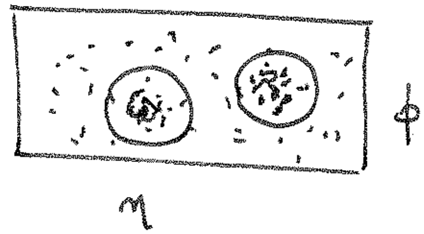

and adjust the positions of the circles to enclose the maximum amount of p_T. The circles are cones in the $(p_T\,\eta\,\phi)$ space. The radius R of the circle in (η, ϕ), which is the radius of the cone, is the resolution parameter: a smaller value of R gives a higher resolution into jets. At the Tevatron, it has been conventional to take $R = 0.7$, but other choices can be used.

Figs p.12, from the review of Campbell, Houston, and Stirling, shows the relation of the cone jet energy to the initial parton energy for $R = 0.7$ cone jets. The parton shower, which produces radiation out of the cone, lowers the cone jet energy. The underlying event adds to the cone jet energy. The two effects approximately balance for $R \sim 0.4$.

A cone jet algorithm must be carefully designed to be infrared safe. The danger is that the cone positions can change qualitatively with soft gluon radiation. Consider, for example, a configuration with two energetic jets of particles separated by $\Delta R \lesssim 1.4$. Usually these would be assigned to separate cones, but radiation of a soft gluon in the middle

might cause the two jets to be included in the same cone. The cone algorithms used by CDF and DØ avoid this difficulty by requiring a minimum p_T in a cone of smaller radius, which is then expanded to $R = 0.7$.

There is also a hadron collider version of the k_T algorithm. This is easier to state than the cone algorithm. We use

$$\hat{y}_{ab} = \min(p_{Ta}^2, p_{Tb}^2) \cdot \Delta R_{ab}^2$$

to order the merger of particles or partons.

As in e^+e^- annihilation, going to higher order in QCD perturbation theory produces new effects not found at the leading order. Figs p. 13 shows an example in a DØ analysis. The figure shows the distribution of $\Delta\phi$ between the two most energetic jets in the event. In 3-jet events, $\Delta\phi > 120°$; otherwise, one of the jets chosen is not the most energetic. The region $\Delta\phi < 120°$ is filled in by 4-parton events that appear at the next order in α_s. The curves show a comparison of

DØ data to an $O(\alpha_s)$ (LO) calculation and to an $O(\alpha_s^2)$ (NLO) calculation by Nagy.

Another effect that arises only at higher orders in α_s is the jet profile. At leading order, the jet is a single parton:

At the next order, collinear radiation from the parton gives the jet a finite size

Gluons have a larger splitting probability than quarks, so gluon jets are predicted to be fatter than quark jets. Figs. p. 14 shows the measurement by CDF of the quantity

$$\psi(r) = \frac{\sum p_T \text{ inside radius } rR}{\sum p_T \text{ inside radius } R} \qquad \text{for } R = 0.7$$

The data is compared to an $O(\alpha_s)$ calculation by Ellis, Kunszt, and Soper. (Because the jet shape arises for the first time at this order in α_s, there is a strong dependence on the renormalization scale.) In the lower part of the figure, we see the dependence of the jet profile on the jet p_T. Jets with higher p_T are narrower, as one might have expected.

Fig. p. 15 shows a very interesting recent analysis of the jet profile from CDF run II data. The data shows the measured value of

$$1 - \Psi(r) \qquad \text{for } R=0.7 \qquad rR = 0.3$$

as a function of p_T. The quantity decreases with p_T. The purple and blue curves are the predictions of the PYTHIA parton shower for quark jets and for gluon jets. The observed decrease is a combination of the narrowing of jets with increased p_T and the transition, at the $p\bar{p}$ collider, from gluon jets to quark and antiquark jets as p_T increases.